

Antimalarial Pyrido[1,2-*a*]benzimidazoles: Lead Optimization, Parasite Life Cycle Stage Profile, Mechanistic Evaluation, Killing Kinetics, and in Vivo Oral Efficacy in a Mouse Model

Kawaljit Singh,^{†,‡} John Okombo,[†] Christel Brunschwig,^{||} Ferdinand Ndubi,[†] Linley Barnard,[†] Chad Wilkinson,[†] Peter M. Njogu,[§] Mathew Njoroge,^{||} Lizahn Laing,^{||} Marta Machado,[⊥] Miguel Prudêncio,[⊥] Janette Reader,[#] Mariette Botha,[#] Sindisiwe Nondaba,[#] Lyn-Marie Birkholtz,[#] Sonja Lauterbach,[∇] Alisje Churchyard,[∇] Theresa L. Coetzer,[∇] Jeremy N. Burrows,[○] Clive Yeates,[◆] Paolo Denti,^{||} Lubbe Wiesner,^{||} Timothy J. Egan,^{†,∞} Sergio Wittlin,^{||,∞} and Kelly Chibale^{*,†,‡,∞}

[†]Department of Chemistry, University of Cape Town, Rondebosch 7701, South Africa

[‡]South African Medical Research Council Drug Discovery and Development Research Unit, Department of Chemistry and Institute of Infectious Disease and Molecular Medicine, University of Cape Town, Rondebosch 7701, South Africa

[§]Department of Pharmaceutical Chemistry, University of Nairobi, P.O. Box 19676, Nairobi, 00202, Kenya

^{||}Department of Medicine, Division of Clinical Pharmacology, University of Cape Town, Observatory, 7925, South Africa

[⊥]Instituto de Medicina Molecular, Faculdade de Medicina, Universidade de Lisboa, Av. Prof. Egas Moniz, 1649-028 Lisboa, Portugal

[#]Department of Biochemistry, Institute for Sustainable Malaria Control, University of Pretoria, Private Bag X20, Hatfield 0028, South Africa

[∇]Wits Research Institute for Malaria, Faculty of Health Sciences, University of the Witwatersrand and National Health Laboratory Service, Johannesburg 2193, South Africa

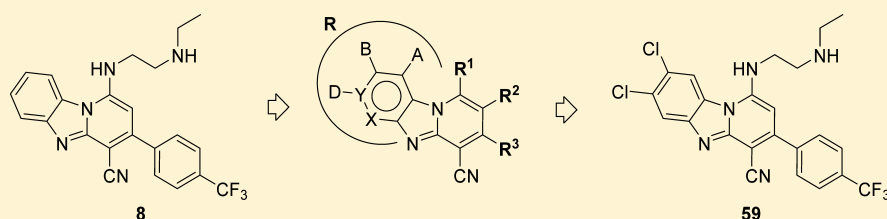
[○]Medicines for Malaria Venture, ICC, Route de Pré-Bois 20, P.O. Box 1826, 1215 Geneva, Switzerland

[◆]Inpharma Consultancy, 6 Dudley Hill Close, Welwyn, Hertfordshire AL60QQ, U.K.

^{||}Swiss Tropical and Public Health Institute, Socinstrasse 57, 4002 Basel, Switzerland

[∞]University of Basel, 4003 Basel, Switzerland

S Supporting Information



8
IC₅₀ *Pf*NF54 = 120 nM; *Pf*K1 = 110 nM
in vivo *P. berghei* (HCl salt; p.o.) 4×25 mg/kg = 95.7%
0/3 malaria infected mice cured

59
IC₅₀ *Pf*NF54 = 18 nM; *Pf*K1 = 19 nM
in vivo *P. berghei* (p.o.) 4×30 mg/kg = 99.7%
3/3 malaria infected mice cured

ABSTRACT: Further structure–activity relationship (SAR) studies on the recently identified pyrido[1,2-*a*]benzimidazole (PBI) antimalarials have led to the identification of potent, metabolically stable compounds with improved in vivo oral efficacy in the *P. berghei* mouse model and additional activity against parasite liver and gametocyte stages, making them potential candidates for preclinical development. Inhibition of hemozoin formation possibly contributes to the mechanism of action.

INTRODUCTION

Malaria, a parasitic disease caused by parasites of the *Plasmodium* genus, remains a global public health concern due to its morbidity and mortality, with approximately 214 million new clinical cases and about 438 000 deaths reported in 2015.¹ Mammalian infection is initiated by the bite of *Plasmodium*-infected female *Anopheles* mosquitoes. An asymptomatic but obligatory developmental phase in the liver ensues, leading to the release of newly formed parasites into the bloodstream, where they infect

red blood cells and cause disease symptoms.² Transmission of the parasite to the mosquito vector occurs when the latter ingests circulating gametocytes, initiating the sexual stage of the parasite's life cycle. Chemotherapy represents one of the most effective control measures to mitigate the malaria burden, with the World Health Organization (WHO) presently recommending

Received: November 9, 2016

Published: January 17, 2017

the use of artemisinin combination therapies (ACT) for treatment of uncomplicated malaria. However, there is compelling evidence from Southeast Asia describing the emergence and spread of ACT tolerance, which is characterized by reduced clearance rates of *Plasmodium falciparum* parasites.^{3,4} This underscores the urgent need to expand the antimalarial drug arsenal by exploring and developing new compound classes, preferably with a combination of novel modes of action, multistage activity, good safety profile, and efficacy at low doses.

The benzimidazole motif is a recognized privileged scaffold in medicinal chemistry due to its capacity to interact with numerous biological systems,⁵ leading to a wide variety of biological activities, including antimalarial activity.^{6–9} Pyrido-[1,2-*a*]benzimidazoles (PBIs), previously investigated for antibacterial, antifungal, antiviral, and antitumor activities,¹⁰ were recently shown to be a novel antimalarial chemotype.¹¹ The lead compound from the previous studies, **8** (Figure 1),

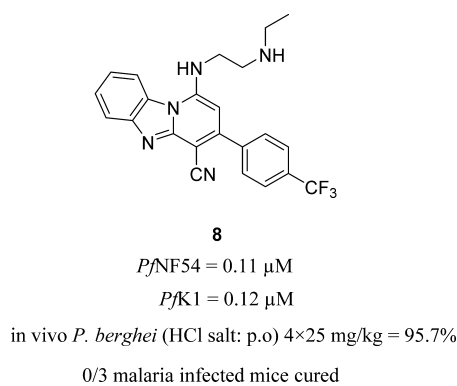


Figure 1. Original lead compound **8**, with activity against chloroquine-sensitive ($PfNF54$) and chloroquine/multidrug-resistant ($PfK1$) *P. falciparum* strains.¹¹

showed high antiplasmodial activity in vitro ($IC_{50}(PfNF54) = 0.11 \mu\text{M}$; $IC_{50}(PfK1) = 0.12 \mu\text{M}$) and promising oral efficacy (96% at $4 \times 50 \text{ mg/kg p.o.}$) in vivo in the rodent *P. berghei* model. However, pharmacokinetic (PK) studies indicated saturation in oral absorption at low doses, presumably due to poor dissolution or solubility, which may be a factor in limiting oral efficacy. Herein, we describe further structure–activity relationship (SAR) investigations (SAR_{1–4}) around the scaffold

of compound **8** (Figure 2), partly to explore the potential for generating derivatives with an improved PK profile but also to explore the effect on activity of changes around parts of the scaffold not previously investigated, with the goal of improving oral activity in the mouse model to confirm if this series has potential for further development.

The SAR studies can be broken down according to Figure 2:

- SAR₁—replacement of the alkylamino side chain with various alkyl, cycloalkyl, and heterocyclic moieties containing water-solubilizing H-bonding groups, encompassing hydroxypyrrolidine, azetidinol, hydroxypiperidine, piperazine or sulfonamide substituents;
- SAR₂—introduction of small hydrophobic substituents at the C-2 position to favor non-coplanar conformations of the C-3 aryl, lowering the crystal packing energies and consequently improving aqueous solubility,¹²
- SAR₃—replacement of the 4-trifluoromethylphenyl (4-CF₃Ph) at the C-3 position with substituted or unsubstituted phenyl rings and with saturated systems or cycloalkyl groups and introduction of water-solubilizing H-bonding groups including ester, sulfinyl, sulfone, and sulfoxide substituents on the C-3 phenyl ring;
- SAR₄—introduction of substituents on the previously¹¹ unexplored left aromatic ring, including replacement with the less lipophilic pyridyl ring.

The in vitro antiplasmodial activities of synthesized derivatives against chloroquine-sensitive (CQS) and multidrug-resistant *P. falciparum* strains as well as in vivo efficacy in *P. berghei*-infected mice are reported. Additionally, we present metabolic stability, killing kinetics, and gametocytocidal and liver stage activity data on a subset of the compounds. Some mechanistic studies were done, focusing on the potential for inhibition of hemozoin (Hz) formation, on the hypothesis that the ability of PBIs to adopt flat conformations would allow for π – π stacking interactions with ferriprotoporphyrin IX (Fe(III)PPIX), a toxic byproduct of host hemoglobin degradation, thus leading to inhibition of Hz crystal formation and consequent parasite death.

RESULTS AND DISCUSSION

Chemistry. The synthesis of target PBI derivatives was relatively straightforward using published procedures (Scheme 1).¹¹

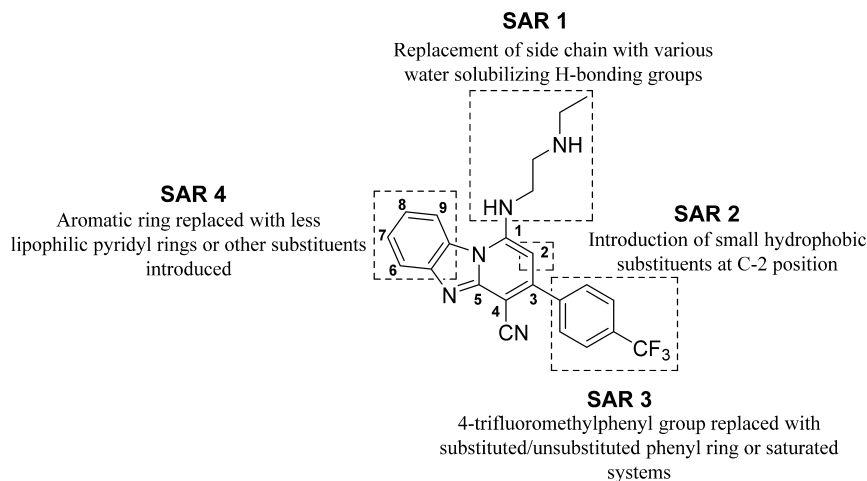
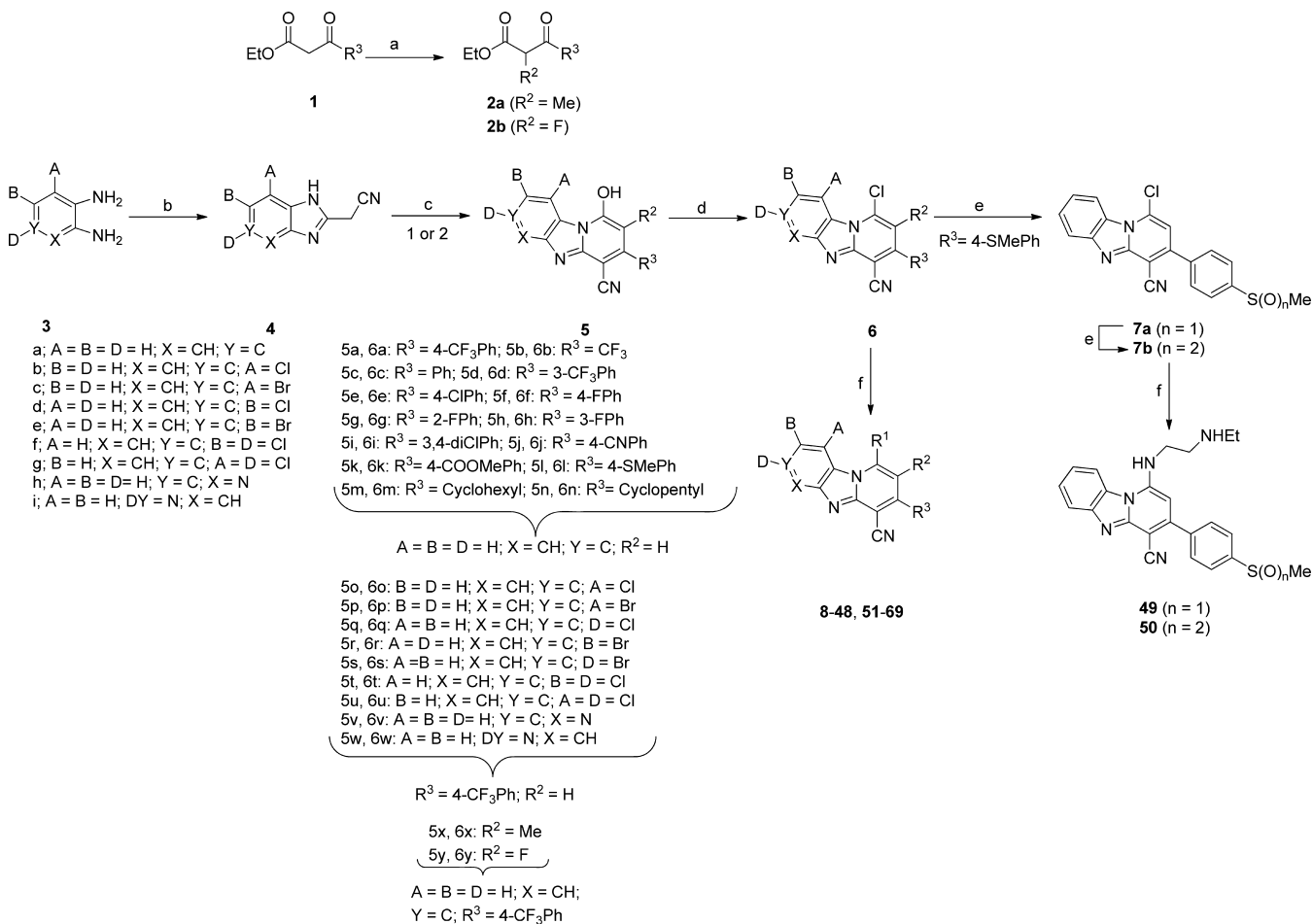


Figure 2. SAR explorations around lead compound **8**.

Scheme 1. Synthesis of Pyrido[1,2-*a*]benzimidazole Derivatives^a

^aReagents and conditions. (a) For $R^2 = \text{Me}$: MeI, K_2CO_3 , MeCN, 50°C , 2 h (**2a**, 52%). For $R^2 = \text{F}$: Selectfluor, MeCN, microwave (150 W), 82°C , 10 min (**2b**, 66%). (b) Ethyl cyanoacetate, DMF, microwave, 110°C , 15–45 min; (c) NH_4OAc , 150°C , 1 h; (d) POCl_3 , 130°C , 2 h; (e) *m*CPBA, DCM, 0°C , 1.5 h; (f) amine, Et_3N , THF, 80°C , microwave, 20 min. R^1 as defined in Tables 1 and 3.

Biology: In Vitro Antiplasmodial Activity and Cytotoxicity. All compounds were evaluated for in vitro antiplasmodial activity against the CQS *PfNF54* strain; those with submicromolar activity (34/62 compounds) were further tested against the multidrug resistant *PfK1* strain and for mammalian cytotoxicity against Chinese hamster ovary (CHO) cell lines. The results are summarized in Tables 1–3. In general, activity of the compounds were $0.02\text{--}0.95\ \mu\text{M}$ and $0.02\text{--}1.07\ \mu\text{M}$ against *PfNF54* and *PfK1*, respectively, with 28/34 exhibiting submicromolar potency against both strains.

With regard to SAR, the following observations were made.

(1) For SAR_1 , with variation in the aminoalkyl side chain, with heterocyclic, cyclic, and alkyl substituents containing H-bonding groups (9–38; Table 1):

- The only improvement in vitro was found in replacement of the *N*-ethyl in **8** with a 3-hydroxy pyrrolidyl side chain (**11**), showing $\sim 3\times$ reduction in IC_{50} relative to **8**, with better selectivity.
- Introduction of the same side chain present in chloroquine (**16**, **17**) resulted in a significant drop in activity and poor selectivity.

(2) For SAR_2 , with introduction of $-\text{Me}$ or $-\text{F}$ substituents at C-2 (**66–69**; Table 3):

- Retaining the *N*-ethyl ethylenediamine side chain of **8** and introducing a C-2 Me (**66**) or F (**67**) resulted in a

significant loss in activity, with a 10–50 \times increase in *PfNF54* IC_{50} .

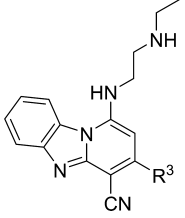
- Activity of the 2-Me and 2-F derivatives was improved by introduction of the 3-hydroxypyrrolidyl side chain (**68**, **69**), consistent with the previous observations from SAR_1 (see **11**; Table 1), with the 2-F analogue (**69**) now showing comparable activity to **8** with significantly better selectivity.

(3) For SAR_3 , with replacement of the 4- CF_3Ph in **8** with unsubstituted and substituted phenyl rings and cycloalkyl groups (**39–53**; Table 2):

- Varying the position of the $-\text{CF}_3$ group from the para (**8**) to the meta-position (**40**) had only a slight effect on activity. The unsubstituted phenyl and a range of ortho (**43**), meta (**44**), para (**41**, **42**, **46**, **50**), and disubstituted derivatives (**45**) all retained significant activity (*PfNF54* $\text{IC}_{50} < 1\ \mu\text{M}$), with only **50** showing a significant improvement in selectivity.
- Substitution with a para $-\text{COOMe}$ (**47**), $-\text{SMe}$ (**48**), or $-\text{SOMe}$ (**49**) significantly lowered activity, as did replacing the 4- CF_3Ph with a $-\text{CF}_3$ (**51**).
- Cycloalkyl groups at C-3, including cyclohexyl (**52**) and cyclopentyl (**53**), were well tolerated but showed no improvement in selectivity.

Table 1. In Vitro Antiplasmodial Evaluation of Pyrido[1,2-*a*]benzimidazoles 8–38 (SAR₁)

Compound	R ¹	R ³	Antiplasmodial Activity, ^{a,b} IC ₅₀ (μM)		Cytotoxicity	
			<i>Pf</i> NF54	<i>Pf</i> K1	CHO ^c IC ₅₀ (μM)	SI
8			0.12	0.11	1.56	13
9			0.39	0.79	10.50	27
10			5.99			
11			0.04	0.03	6.12	153
12			1.10			
13			>10			
14			9.10			
15			16.42			
16			4.13			
17			0.69	0.40	2.91	4
18			>24			
19			8.48			
20			0.44	1.00	5.98	14
21			0.70	0.96	4.07	6
22			1.38			
23			4.42			
24			0.84	0.90	6.31	8
25			21.32			

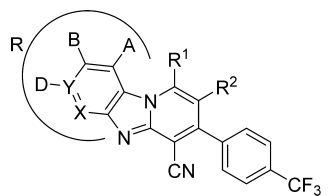
Table 2. In Vitro Antiplasmodial Evaluation of Pyrido[1,2-*a*]benzimidazoles 39–53 (SAR₃)


Compound	R ³	Antiplasmodial Activity ^{a, b}		Cytotoxicity	
		IC ₅₀ (μM)		CHO ^c IC ₅₀ (μM)	SI
		<i>Pf</i> NF54	<i>Pf</i> K1		
8		0.12	0.11	1.56	13
39		0.70	1.07	18.30	26
40		0.21	0.34	5.92	28
41		0.66	0.43	9.60	15
42		0.33	0.54	11.50	35
43		0.89	1.00	24.40	27
44		0.38	1.00	5.18	13
45		0.11	0.12	1.55	14
46		0.17	0.20	3.90	23
47		1.56			
48		3.90			
49		3.81			
50		0.31	0.33	204	658
51		2.93			
52		0.47	0.67	3.19	7
53		0.83	0.82	3.77	5
Emetine				0.095	

^aMean from *n* values of ≥ 2 independent experiments with multidrug resistant (K1) and CQ-sensitive (NF54) strains of *P. falciparum*. ^bChloroquine (CQ) and artesunate (AS) were used as reference drugs in all experiments. Against *Pf*NF54 and *Pf*K1, our laboratory standard IC₅₀ values for CQ and AS are 0.016 μM/0.194 μM and 0.004 μM/0.003 μM (mean from ≥ 10 independent assays). ^cCHO = Chinese hamster ovarian cells. SI = selectivity index = [IC₅₀(CHO)/IC₅₀(*Pf*NF54)].

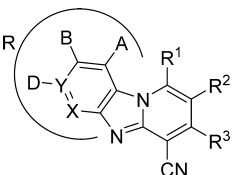
- Predicted lipophilicity was relatively high (log *P* > 3 for most compounds). For SAR₁ and SAR₃ analogues, increased lipophilicity was associated with better permeability while lower lipophilicity was associated with

better solubility, except for 17 with high log *P* but good solubility. There was no apparent relationship between lipophilicity and metabolic stability for this series of compounds, suggesting that structural changes

Table 3. In Vitro Antiplasmodial Evaluation of Pyrido[1,2-*a*]benzimidazoles 54–69 (SAR₂)


Compound	R	R ¹	R ²	Antiplasmodial Activity ^{a, b} IC ₅₀ (μM)		Cytotoxicity	
				<i>Pf</i> NF54	<i>Pf</i> K1	CHO ^c IC ₅₀ (μM)	SI
8			H	0.12	0.11	1.56	13
54			H	0.03	0.03	8.71	362
55			H	0.38		1.80	5
56			H	0.07		4.44	63
57			H	0.14	0.26	1.63	5
58			H	0.15	0.24	1.55	2
59			H	0.02	0.02	3.39	188
60			H	0.03	0.04	11.20	431
61			H	0.05	0.19	4.19	6.1
62			H	0.26		5.90	22.3
63			H	0.18	0.21	2.98	7.3
64			H	0.14	0.13	4.10	5
65			H	0.27	0.84	3.14	6
66			Me	1.28			
67			F	5.53			
68			Me	0.55	0.47	25.0	45
69			F	0.19	0.17	206	1084
Emetine						0.095	

^aMean from *n* values of ≥ 2 independent experiments with multidrug resistant (K1) and CQ-sensitive (NF54) strains of *P. falciparum*. ^bChloroquine (CQ) and artesunate (AS) were used as reference drugs in all experiments. Against *Pf*NF54 and *Pf*K1, our laboratory standard IC₅₀ values for CQ and AS are 0.016 μM/0.194 μM and 0.004 μM/0.003 μM (mean from ≥ 10 independent assays). ^cCHO = Chinese hamster ovarian cells. SI = selectivity index = [IC₅₀(CHO)/IC₅₀(*Pf*NF54)].

Table 4. Physicochemical Properties and in Vitro Microsomal Stability of Selected Pyrido[1,2-*a*]benzimidazoles


Compound	R	R ¹	R ²	R ³	LogP ^b	Melting Point (°C)	Kinetic Solubility (μM)	Permeability (log P _{app} class) ^c		Met Stability (% remaining after 30 min)	
								pH6.5	pH4.0	pH6.5	MLMs
8			H		4.7	222–224	<5	-6.9, low	-4.3, high	97	84
11			H		4.0	267–269	<5	-7.2, low	-4.9, high	51	
12			H		4.1	310–312	<5				
17			H		6.2	220–222	85	-6.4, mod	-3.5, high	32	53
20			H		4.6	215–217	<5	-7.0, low	-3.8, high	63	75
26			H		4.3	>270				65	99
36			H		4.5	233–235	<5		-5.7, mod	92	91
44			H		3.9	203–205	25	-7.1, low	-5.0, high	100	89
45			H		4.8	235–237				65	60
50			H		2.4	227–230	40	-6.4, mod	-6.7, low	86	
52			H		4.0	216–218	10			42	
54			H		5.2	224–227				75	87
57			H		5.2	223–225	10	-7.2, low	-4.0, high	93	89
59			H		5.8	305–307	10		-6.5, mod	81	95
60			H		5.8	319–321	20		-4.9, high	87	87
64			H		4.5	225–227	10		-4.2, high		
66			Me		5.1	236–238	<5		-5.4, high	80	85

Table 4. continued

Compound	R	R ¹	R ²	R ³	LogP ^b	Melting Point (°C)	Kinetic Solubility (μM)	Permeability (log P _{app} class) ^c		Met Stability (% remaining after 30 min)		
								pH4.0	pH6.5	MLMs	HLMs	
67			F		4.8	293–295	160		-5.2, high	35	39	
68			Me		4.5	236–238	<5		-3.9, high			
69			F		4.2	265–267	80		-5.3, high	37		
Warfarin									-3.7, high	-3.8, high		
Propranolol									-5.9, mod	-4.4, high		
Testosterone									-3.8, high	-3.7, high		
Midazolam											1.3	0.1
MMV390048 ^a											94	93

^aReference 26. (3-[2-(Trifluoromethyl)pyridin-5-yl]-5-[4-(methylsulfonyl)phenyl]pyridin-2-amine. ^bPredicted from ChemBioDraw Ultra, version 14.0. ^cLow permeability, log P_{app} < -6.5; moderate permeability (mod), log P_{app} from -6.5 to -5.5; high permeability, log P_{app} > -5.5.

had a greater contribution to these properties than lipophilicity.

Metabolic Stability in Liver Microsomes (Table 4). The most active compounds in the in vitro antiplasmodial assay were assessed for metabolic stability in mouse and human liver microsomes (MLMs and HLMs, respectively). Most compounds showed no significant interspecies difference in microsomal stability, and the following trends were observed:

- Introduction of a piperidinyl (20, 26) or CQ-like side chain (17) led to a significant decrease in microsomal stability, with the exception of 36, where the piperidinyl ring was directly linked to the PBI scaffold.
- 2-Methyl substitution (SAR₂) was not detrimental to microsomal stability (66), but surprisingly the 2-F analogue (67) was significantly less stable.
- Variation in the substitution on the C-3 aryl (SAR₃) had a significant effect on stability, with the dichloro derivative (45) showing significantly poorer stability compared to 8.
- The more active compounds with halogen substitution on the benzimidazole (SAR₄; 54, 57, 59, 60) did not show any significant difference in microsomal stability relative to 8.

In Vivo Efficacy in the Mouse *P. berghei* Model (Table 5).

Compounds with good antiplasmodial activity, reasonable solubility, and high microsomal stability were assessed for in vivo efficacy in *P. berghei*-infected mice, dosing orally at 4 × 50 mg/kg. If mice were cured, lower doses were evaluated (4 × 30 mg/kg, 4 × 10 mg/kg, and 4 × 3 mg/kg). Parasitemia reduction in *P. berghei* in vivo efficacy testing helped to efficiently prioritize compounds in the knowledge that those with good efficacy must have exposure. PK was followed up in detail on those that were most interesting. In summary, the following observations were made.

- Compound 44, less active than 8 in vitro but with slightly superior microsomal stability, showed slightly better in vivo efficacy compared to 8, with a single cure at 4 × 50 mg/kg.

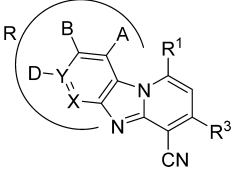
- Compound 57, with comparable in vitro activity and microsomal stability to 8, was not curative at 4 × 50 mg/kg.
- Compounds 59 and 60, with significantly better in vitro activity and comparable microsomal stability to 8, were completely curative at 4 × 50 mg/kg, 59 proving better at 4 × 30 mg/kg. At lower doses (4 × 10 mg/kg and 4 × 3 mg/kg), the mice were not cured (MSD of 16–18) although parasitemia was still reduced by >99%.

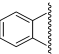
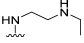
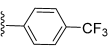
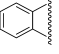
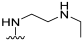
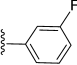
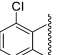
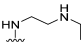
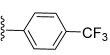
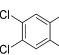
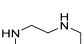
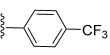
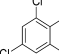
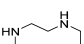
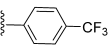
Pharmacokinetic Studies (Table 6). Studies were performed in mice dosed orally (p.o.) at 10 mg/kg and intravenously (iv) at 2.5 mg/kg with compounds 59 and 60 (Figure 3). Since the elimination phase was not captured in the standard 24 h sampling period and noncompartmental analysis could not provide reliable parameter estimates, both iv and oral data were interpreted with nonlinear mixed-effects modeling where a two-compartment disposition model was used, with first-order absorption and elimination; bioavailability was assumed 100% for the iv dose and estimated for the oral formulation. Between-mouse variability was included in the absorption rate constant, plasma clearance, and oral bioavailability. The PK parameters from the model were used to derive the exposure metrics in Table 6.

Both 59 and 60 were slowly absorbed when dosed orally (T_{max} of ≥10 h) and were slowly eliminated (i.e., CL < 30 mL min⁻¹ kg⁻¹). Considered in relation to the previous PK studies on 8,¹¹ which showed broadly similar pharmacokinetics to 59 and 60, it would appear that the significant improvement in efficacy of 59 and 60 in *P. berghei*-infected mice is likely to be due more to their better inherent antimalarial activity than improved pharmacokinetics.

Gametocytocidal and Liver Stage Activity (Table 7).

The potential of this compound class to act as dual- or triple-action antimalarials was determined by evaluating their gametocytocidal potency¹³ and liver stage activity. Compound 8 and a range of 17 new analogues were tested against early (EG; >90% stage II/III) and late (LG; >95% stage IV/V) gametocytes. The potential for inhibition of liver stage *Plasmodium* infection was assessed using a model with a *P. berghei* infected human hepatoma cell line (HuH 7).¹⁴ Compounds 54 and 59,

Table 5. In Vivo Oral Efficacy of Selected Pyrido[1,2-*a*]benzimidazoles in *P. berghei*-Infected Mice


Code	R	R ¹	R ³	<i>Pf</i> /NF54 IC ₅₀ (μ M)	Oral Dose ^a (mg/kg)	% Reduction in parasitemia (MSD) ^b	Cured/ Infected
8				0.12	4 x 50	96.0 (14) ^c	0/3
					4 x 25	96.0 (14) ^c	0/3
					4 x 12.5	81.0 (14) ^c	0/3
					4 x 6	38.0 (7) ^c	0/3
					4 x 3	0 (4) ^{c,d}	0/3
44				0.38	4 x 50	61.0 (24)	1/3
57				0.14	4 x 50	85.0 (7)	0/3
59				0.02	4 x 50	98.0 (30)	3/3
					4 x 30	99.7 (30)	3/3
					4 x 10	99.6 (18)	0/3
					4 x 3	99.5 (17)	0/3
60				0.03	4 x 50	98.0 (30)	3/3
					4 x 30	99.4 (30)	2/3
					4 x 10	99.4 (18)	0/3
					4 x 3	99.4 (16)	0/3
Chloroquine ^e				0.016	4 x 30	99.9 (24)	0/10
Control					-	-(4) ^d	

^aTest compounds were formulated in 90/10 Tween 80/ethanol (v/v), diluted 10 times with water, and administered orally once per day on 4 consecutive days (4, 24, 48, and 72 h after infection). ^bMSD = mean survival time in days. ^cUsed the HCl salt.¹¹ ^dMice with <40% parasitemia reduction were euthanized on day 4 in order to prevent death otherwise occurring at day 6. ^eData from Le Manach et al., 2014.²⁷

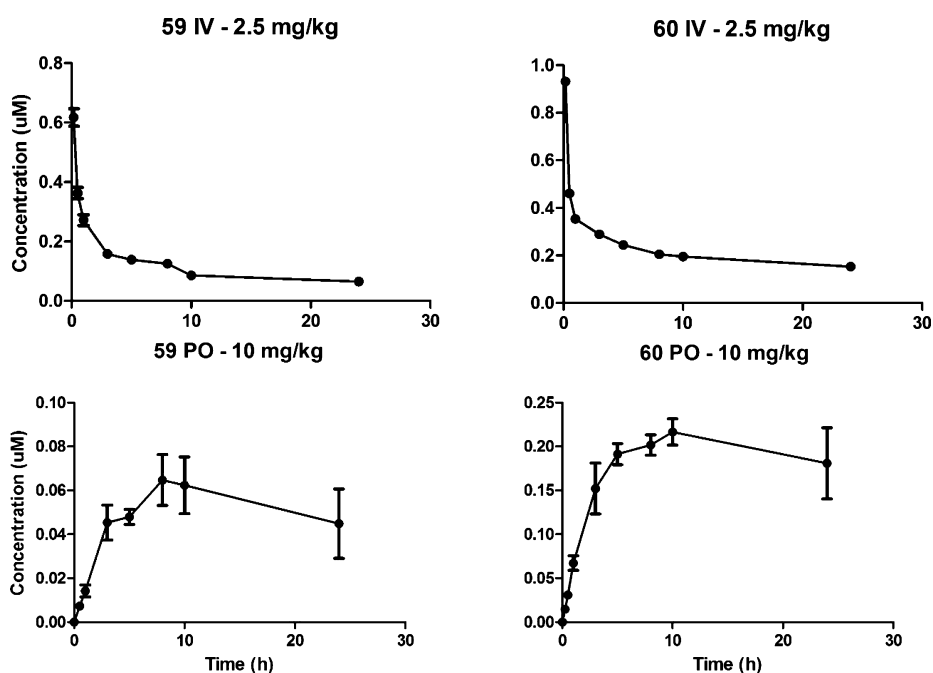
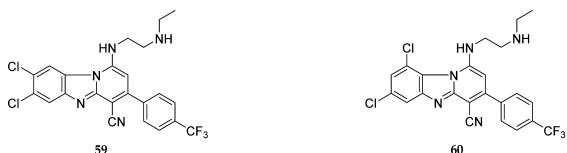


Figure 3. Systemic exposure of 59 and 60 following single intravenous and oral dose administration to healthy mice ($n = 3$).

Table 6. Pharmacokinetic Parameters for 59 and 60 in Mice



Parameter	i.v. (2.5mg/kg) ^a	p.o. (10mg/kg) ^b	i.v. (2.5mg/kg) ^a	p.o. (10mg/kg) ^b
$t_{1/2}$ (h) ^c	15	15	21	21
C_{max} (μ M)	-	0.07	-	0.22
T_{max} (h)	-	10	-	>10
V_d (L/kg) ^c	26	-	19	-
CL (mL/min/kg) ^c	21	-	11	-
$AUC_{0-\infty}$ (μ M/L.min) ^c	256	158	571	686
Oral bioavailability (%) ^c	-	<15	-	30

^aFor intravenous dosing ($n = 3$ mice), compounds were formulated in a solution of dimethylacetamide, polyethylene glycol, and propylene glycol/ethanol mixture 4:1 at a ratio 1:3:6. ^bFor oral dosing ($n = 3$ mice), compounds were formulated as suspension in 100% HPMC. ^cPK exposure parameters derived from the population parameters of the pharmacometric model.

with good in vitro blood stage activity, also showed comparable activity against both EG and LG, while others (8, 42, 52) showed a degree of stage-specific potency for LG gametocytes, indicated by a > 2-fold change in IC_{50} .

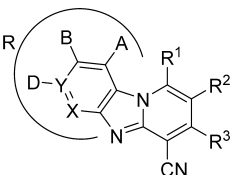
Initial screening at 1 μ M, 5 μ M, and 10 μ M on liver stage infection and cell confluence using luciferase-expressing parasites and a luminescence-based method¹⁵ established the nontoxicity of the test compounds, with no significant effect on cell proliferation. Compounds 26, 66, and 69 led to the strongest decrease in infection at the lowest concentration tested (1 μ M), and a subsequent dose–response analysis confirmed their activity. Compound 69, which also had good blood stage activity ($PfK1$ $IC_{50} = 0.17$ μ M), was the most potent inhibitor in the *P. berghei* liver stage assay ($IC_{50} = 1.42$ μ M), significantly more active than primaquine (PMQ) ($IC_{50} = 8.42$ μ M), albeit less active than atovaquone ($IC_{50} = 1.1$ nM).¹⁶ It should be noted that PMQ's activity in vivo is dependent on its oxidation to active metabolites¹⁷ and, as such, the compound's IC_{50} in vitro does not necessarily represent its in vivo potency. Compounds 26 ($IC_{50} = 3.31$ μ M) and 66 ($IC_{50} = 2.85$ μ M) also showed a degree of activity in the in vitro liver stage assay, in addition to their blood stage activity.

Speed of Action. There was a suspicion from the previous studies on 8 in the *P. berghei* mouse model that the compounds might be inherently slow acting. To investigate this further, a cross section of nine compounds were run through a [³H]hypoxanthine incorporation assay designed to assess their killing speed at 24, 48, and 72 h.¹⁸ The IC_{50} values of pyrimethamine, 11, and 69 were respectively 6-, 18-, and 22- fold higher at 24 h compared to 72 h (Figure 4), indicating that these compounds were slow acting; it may be noteworthy that 11 and 69 have the 3-hydroxypyrrolidinyl side chain. However, 8, 20, 17, and 44 appeared to be faster acting ($IC_{50}(24\text{ h})/IC_{50}(72\text{ h}) < 1.5$), comparable to CQ and AS, while 9, 54, and 59 could be classified as neither fast nor slow, with $IC_{50}(24\text{ h})/IC_{50}(72\text{ h}) = 1.5$ –2. Overall, albeit based on the relatively few compounds tested, it appears that there was neither a bias for any particular killing speed nor significant correlation between speed of action and the previously quoted in vitro efficacy against *PfNF54*.

Mechanistic Studies. Due to their structural likeness to CQ, which includes a planar heterocyclic moiety, a halo substitution, and a basic amine side group, the mechanistic

potential of these compounds to inhibit Hz formation was investigated by measuring their ability to inhibit in vitro β -hematin (β H) formation. Although a number of these derivatives were able to inhibit β H formation ($IC_{50} < 100$ μ M) in a detergent-mediated Nonidet P-40 (NP-40) assay (Supporting Information Table S1), there was only a weak, albeit statistically significant, linear correlation with whole-cell activity against *PfNF54* (Figure 5). It is possible that the cell-free β H inhibition assay does not mirror the cellular Hz inhibitory activity or that there is only weak drug–heme complex formation due to poor binding to free heme molecules or that Hz inhibition is not the sole target of this class of compounds.

To confirm if these compounds were bona fide inhibitors of Hz formation, a cellular fractionation assay was used to determine free heme and Hz signatures when synchronized ring stage parasites were treated with increasing doses; for true inhibitors there is a dose-dependent increase in toxic free heme and corresponding decreases in Hz.¹⁹ Of the cross section of compounds studied, 8, 9, 54, and 45 were β H inhibitors in the NP-40 assay ($BHIA_{IC50} < 45$ μ M) while the inactive 69 ($BHIA_{IC50} = 120$ μ M) represented a negative control. No significant changes in toxic free heme or Hz levels with increasing drug concentrations were observed for 69 (Figure 6), while 8 and 45 showed significant concentration-dependent increases in free heme and corresponding decreases in Hz compared to the untreated control, with the free heme and parasite survival curves crossing close to the IC_{50} values of the compounds (Figure 6), a trend not shown by 9 or 54 despite their potency in the NP-40 assay (Supporting Information Figure S1). In silico simulations of vacuolar accumulation of these compounds showed that they are likely to accumulate poorly within the digestive vacuole compared to standard Hz inhibitors (Supporting Information Table S1). Taken together, these studies suggest that inhibition of Hz formation is one but perhaps not the sole or primary target of this class of compounds; their flat conformation possibly allows for weak heme–drug complex formation through only π – π interactions as was recently reported for certain benzamide analogues.²⁰ This would be unlike halofantrine and quinine, for instance, which reportedly require hydrogen bonding and coordination to Fe(III)PPIX in addition to π – π interactions.^{21,22} The lack of β H inhibition by 69 could be ascribed to

Table 7. In Vitro Activity against *Pf*NF54 Gametocytes and *P. berghei* Liver Stage^f


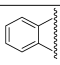
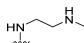
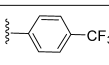
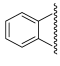
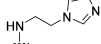
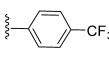
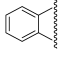
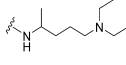
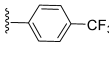
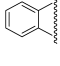
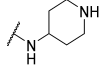
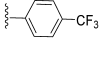
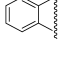
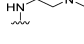
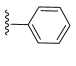
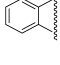
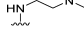
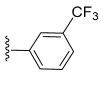
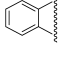
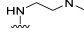
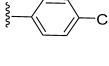
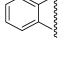
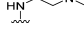
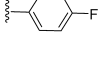
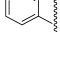

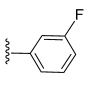
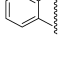
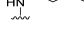
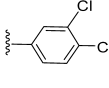
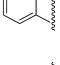
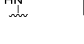
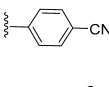
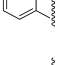

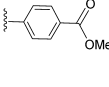
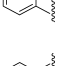

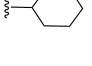
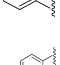

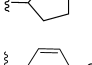
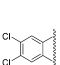
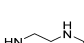
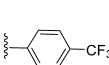
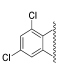
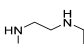
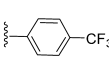
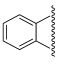
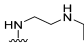
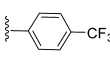



Compound	R	R ¹	R ²	R ³	LG gametocyte IC ₅₀ (μM) ^a	Fold Change ^d (stage preference EG ^c /LG)	<i>P. berghei</i> Liver IC ₅₀ (μM)	<i>Pf</i> NF54 IC ₅₀ (μM)
8			H		0.62 ^b	2.4 (LG)		0.12
9			H		1.02	1.1 (LG)		0.39
17			H		3.02	0.7 (EG)		0.69
26			H		1.16	1.6 (LG)	3.31	0.36
39			H		1.44	-		0.70
40			H		0.49	1.6 (LG)		0.21
41			H		0.69	1.5 (LG)		0.66
42			H		1.77	2.1 (LG)		0.33
44			H		3.63	1.2 (LG)		0.38
45			H		0.59	1.2 (LG)		0.11
46			H		2.66	1.3 (LG)		0.17
47			H		1.68	1.4 (LG)		1.56
52			H		0.46	3.3 (LG)		0.47
53			H		0.67	1.7 (LG)		0.83
54			H		0.82 ^b	1.1 (LG)		0.03
59			H		0.72	1.2 (LG)		0.02
60			H		1.44 ^b	1.2 (LG)		0.03
66			Me		2.57	0.8 (EG)	2.85	1.28

Table 7. continued

Compound	R	R ¹	R ²	R ³	LG gametocyte IC ₅₀ (μM) ^a	Fold Change ^d (stage preference EG ^c /LG)	<i>P. berghei</i> Liver IC ₅₀ (μM)	<i>PfNF54</i> IC ₅₀ (μM)
69			F		-	-	1.42	0.19
MB					0.14			
PMQ							8.42	
ATQ							0.001 ^e	

^aLG (late stage IV/V gametocytes) data were generated using the ATP assay. ^bData generated using the luciferase reporter assay. ^cEG = early gametocytes (stage II/III). LG = late stage IV/V gametocytes. ^dData generated in parallel assays with the luciferase reporter assay, stage preference = EG/LG IC₅₀. ^eData adopted from ref 16. ^fMB = methylene blue. PMQ = primaquine. ATQ = atovaquone.

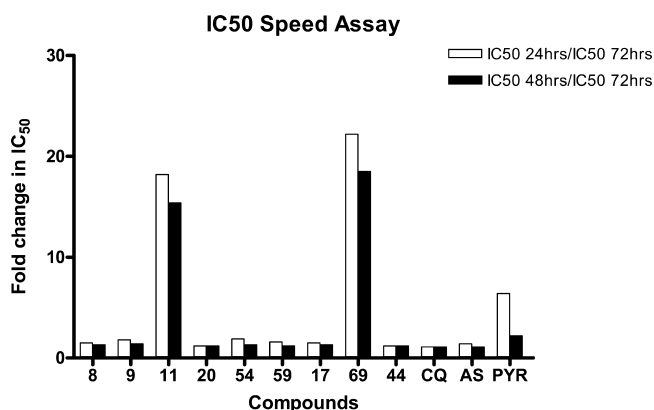


Figure 4. Change in activity of compounds at different assay durations relative to 72 h assay.

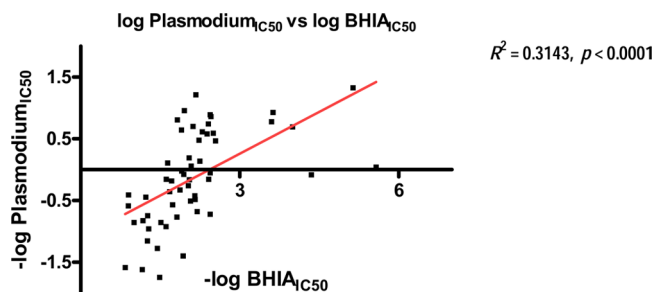


Figure 5. Linear correlation between the inverse of the β H and parasite growth IC₅₀ values for *PfNF54*. Measurements of β H and parasite growth inhibitions were both done in triplicates.

disrupted planarity (from the 2-F substitution) which potentially minimizes π - π interaction.

This leaves the intriguing prospect that the PBIs could act, at least in part, through an as yet unidentified mechanism. Among the diverse activities reported for other pyrido[1,2-*a*]benzimidazoles is the inhibition of the pore-forming protein perforin in mammalian cells by 1-amino-2,4-dicyanopyrido[1,2-*a*]benzimidazoles.²³ This is interesting as the *P. falciparum* proteome harbors perforin-like proteins (PLPs) known to be involved in permeabilizing the erythrocyte membrane during egress of either gametocytes or merozoites.²⁴ A hydroxy derivative 2-ethyl-1-hydroxy-3-methylpyrido[1,2-*a*]benzimidazole-4-carbonitrile (GNF7686) with potent in vitro activity against *Trypanosoma cruzi*, was also recently shown to act through inhibition of cytochrome *b* (a component of cytochrome *bc1* or complex III)²⁵ and a well-established antimalarial target.

While the related hydroxy intermediates from our studies did not show significant antiplasmodial activity (unpublished data), this potential target warrants further investigation as a possible mode of action and encourages further testing for potential activity against kinetoplastids, including *Leishmania donovani*.

CONCLUSIONS

Further SAR studies, aided by physicochemical evaluation and microsomal stability studies, on the antimalarial activity of pyrido[1,2-*a*]benzimidazoles have led to a number of compounds with improved in vitro activity against *P. falciparum*, with substitution on the benzimidazole phenyl being a key factor in improving in vitro activity. Among the most active compounds in vitro, 59 and 60 showed significantly better in vivo activity in the mouse *P. berghei* model. The most active compounds also showed good activity against gametocytes, indicative of potential as dual-acting antimalarials. Other analogues have shown activity against the liver stage of *P. berghei*. There is no conclusive evidence for their mode of action, although inhibition of Hz formation is identified as a potential contributory factor.

EXPERIMENTAL SECTION

All commercially available chemicals were purchased from either Sigma-Aldrich or Combi-Blocks. All solvents were dried by appropriate techniques. Unless otherwise stated, all solvents used were anhydrous. ¹H NMR spectra were recorded on a Varian Mercury spectrometer at 300 MHz or a Varian Unity spectrometer at 400 MHz. ¹³C NMR spectra were recorded at 75 MHz on a Varian Mercury spectrometer or at 100 MHz on Varian Unity spectrometer. Chemical shifts (δ) are given in ppm downfield from TMS as the internal standard. Coupling constants, *J*, are recorded in hertz (Hz). High-resolution mass spectra were recorded on a VG70 SEQ micromass spectrometer. Melting points were determined by differential scanning calorimetry (DSC) using TA Q200/Q2000 DSC from TA Instruments. Analytical thin-layer chromatography (TLC) was performed on aluminum-backed silica gel 60 F₂₅₄ (70–230 mesh) plates. Column chromatography was performed with Merck silica gel 60 (70–230 mesh). Purity was determined by HPLC, and all compounds were confirmed to have >95% purity. The data that are not shown below are supplied in the Supporting Information.

General Procedure for the Synthesis of Compound 4. A mixture of the substituted diaminobenzene 3 (10 equiv) and ethyl cyanoacetate (2.0 equiv) in DMF (1 mL) was heated in a microwave reactor at 110 °C for 15–45 min. The reaction mixture was then diluted with ethyl acetate (20 mL) and washed with water (3 × 15 mL). The organic phase was separated, dried over MgSO₄, filtered and solvent removed under reduced pressure and purified through column chromatography using MeOH/DCM as eluent to afford compound 4.

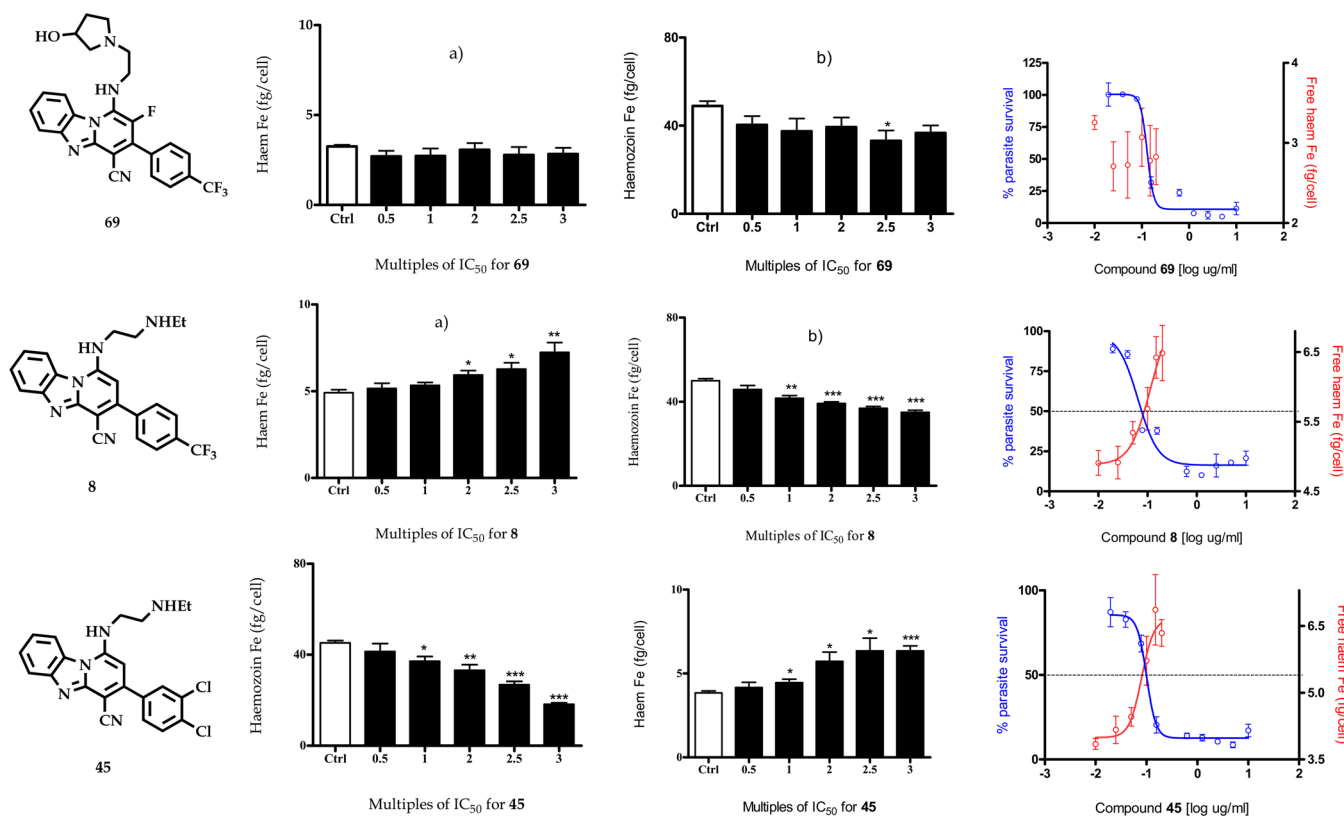


Figure 6. Heme species/fractions in synchronized drug-treated and control *PfNF54* parasites. Plots a and b respectively show free heme and hemozoin represented in terms of iron (Fe) measured in fg/cell with asterisks indicating statistical significance relative to control ($*$) $p < 0.05$; ($**$) $p < 0.01$, and ($***$) $p < 0.001$. Parasite survival (blue) overlaid against free heme Fe (red) plots show an unambiguous trend of increasing level of free heme corresponding with parasite death only in hemozoin inhibitors (c, right-hand column of graphs).

2-(4-Chloro-1H-benzo[d]imidazol-2-yl)acetonitrile 4b. Yellow solid (49%). $R_f = 0.5$ (65% EtOAc–hexane). Mp 190–192 °C. $^1\text{H NMR}$ (400 MHz, DMSO- d_6) δ 7.21 (m, 3H), 5.20 (br s, 1H), 3.89 (s, 2H). $^{13}\text{C NMR}$ (100 MHz, DMSO- d_6) δ 146.3, 140.0, 136.1, 127.3, 125.7, 123.8, 121.9, 116.8, 116.4. MS: LC–MS (ESI) $^+$, found m/z 191.2 [M^+]:193.4 [$\text{M} + 2$] $^+$ (3:1) (calculated for $\text{C}_9\text{H}_6\text{ClN}_3$, 191.62).

2-(3H-Imidazo[4,5-b]pyridin-2-yl)acetonitrile 4i. Brown solid (97%). $R_f = 0.3$ (10% MeOH–DCM). Mp 172–174 °C. $^1\text{H NMR}$ (400 MHz, DMSO- d_6) δ 13.17 (br s, 1H), 8.34 (m, 1H), 7.99 (m, 1H), 7.24 (m, 1H), 4.45 (s, 2H). $^{13}\text{C NMR}$ (100 MHz, DMSO- d_6) δ 147.6, 144.2 (2C), 127.2, 118.5 (2C), 116.6, 19.2. MS: LC–MS (ESI) $^+$, found m/z 159.2 [$\text{M} + \text{H}$] $^+$, (calculated for $\text{C}_8\text{H}_6\text{N}_4$, 158.16).

General Procedure for the Synthesis of Compound 5. A mixture of benzimidazole acetonitrile 4 (1.0 equiv), NH_4OAc (2.0 equiv), and the appropriate β -keto ester 2 (1.2 equiv) was heated to reflux at 150 °C for 1 h and then allowed to cool to 100 °C. MeCN (10 mL) was added and the resulting mixture stirred for 15 min, allowed to cool to room temperature, and then cooled on ice. The cold mixture was filtered and the residue washed with cold MeCN (4 \times 10 mL), dried in vacuo, and used in the next step without further purification.

3-(3,4-Dichlorophenyl)-1-hydroxybenzo[4,5]imidazo[1,2-a]pyridine-4-carbonitrile 5i. Silver tan powder (75%). $R_f = 0.7$ (70% EtOAc–hexane). Mp 249–251 °C. $^1\text{H NMR}$ (400 MHz, DMSO- d_6) δ 13.80 (br s, 1H), 8.61 (d, $J = 8.1$ Hz, 1H), 7.90 (d, $J = 2.1$ Hz, 1H), 7.82 (d, $J = 8.1$ Hz, 1H), 7.64 (dd, $J = 8.3, 2.2$ Hz, 1H), 7.58 (m, 2H), 7.41 (t, $J = 8.2$ Hz, 1H), 6.10 (s, 1H). $^{13}\text{C NMR}$ (100 MHz, DMSO- d_6) δ 158.5, 150.2, 147.9, 137.9, 132.8, 132.5 (2C), 131.9, 131.3, 130.5, 129.0, 128.1, 127.3, 123.1, 117.0, 116.7, 112.2, 105.0. MS: LC–MS (ESI) $^+$, found m/z 354.1 [$\text{M} + \text{H}$] $^+$:356.2 [$\text{M} + \text{H} + 2$] $^+$ (3:1) (calculated for $\text{C}_{18}\text{H}_9\text{Cl}_2\text{N}_3\text{O}$, 353.01).

7,8-Dichloro-1-hydroxy-3-(4-(trifluoromethyl)phenyl)benzo[4,5]imidazo[1,2-a]pyridine-4-carbonitrile 5t. Brownish solid (74%). $R_f =$

0.3 (70% EtOAc–hexane). Mp 305–307 °C. $^1\text{H NMR}$ (600 MHz, DMSO- d_6) δ 8.63 (s, 1H), 7.90 (d, $J = 8.2$ Hz, 2H), 7.83 (d, $J = 8.1$ Hz, 2H), 7.72 (s, 1H), 6.02 (s, 1H). $^{13}\text{C NMR}$ (150 MHz, DMSO- d_6) δ 158.5, 151.8, 150.0, 141.7, 130.0, 129.6 (2C), 129.1, 128.1 (2C), 126.0, 125.9, 125.4, 124.0, 123.6, 117.2 (2C), 114.1, 104.2. MS: LC–MS (ESI) $^+$, found m/z 422.1 [$\text{M} + \text{H}$] $^+$:424.3 [$\text{M} + \text{H} + 2$] $^+$:426.4 [$\text{M} + \text{H} + 4$] $^+$ (9:3:1) (calculated for $\text{C}_{19}\text{H}_8\text{Cl}_2\text{F}_3\text{N}_3\text{O}$, 421.00).

General Procedure for the Synthesis of Compound 6. A mixture of compound 5 (1.0 equiv) and POCl_3 (20 equiv) was heated to reflux at 130 °C for 2 h. Excess POCl_3 was removed under reduced pressure and ice-cold water (20 mL) added to the residue, with stirring to yield a precipitate. The mixture was neutralized with saturated NaHCO_3 and filtered. The resultant solid was washed with ice-cold water (4 \times 15 mL), dried in vacuo, and used without further purification.

1-Chloro-3-(3,4-dichlorophenyl)benzo[4,5]imidazo[1,2-a]pyridine-4-carbonitrile 6i. Yellow solid (98%). $R_f = 0.6$ (30% EtOAc–hexane). Mp 260–262 °C. $^1\text{H NMR}$ (400 MHz, DMSO- d_6) δ 8.72 (d, $J = 8.1$ Hz, 1H), 8.09 (s, 1H), 8.03 (d, $J = 2.1$ Hz, 1H), 7.90 (d, $J = 8.1$ Hz, 1H), 7.83 (dd, $J = 8.3, 2.2$ Hz, 1H), 7.73 (t, $J = 2.1$ Hz, 1H), 7.62 (d, $J = 2.1$ Hz, 1H), 7.44 (t, $J = 8.2$ Hz, 1H). $^{13}\text{C NMR}$ (100 MHz, DMSO- d_6) δ 159.5, 152.2, 148.5, 136.7, 132.7, 132.1 (2C), 131.7, 131.2, 130.1, 129.5, 128.8, 127.5, 123.9, 118.1, 116.5, 113.2, 106.0. MS: LC–MS (ESI) $^+$, found m/z 372.4 [$\text{M} + \text{H}$] $^+$:374.3 [$\text{M} + \text{H} + 2$] $^+$:376.4 [$\text{M} + \text{H} + 4$] $^+$ (9:3:1) (calculated for $\text{C}_{18}\text{H}_8\text{Cl}_3\text{N}_3$, 370.98).

1,7,8-Trichloro-3-(4-(trifluoromethyl)phenyl)benzo[4,5]imidazo[1,2-a]pyridine-4-carbonitrile 6t. Brownish solid (97%). $R_f = 0.8$ (70% EtOAc–hexane). Mp 253–255 °C. $^1\text{H NMR}$ (600 MHz, DMSO- d_6) δ 8.86 (s, 1H), 8.34 (s, 1H), 8.03 (m, 4H), 7.70 (s, 1H). $^{13}\text{C NMR}$ (150 MHz, DMSO- d_6) δ 149.5, 149.4, 144.3, 139.1, 135.4, 134.7, 130.9, 130.4, 130.2, 128.9, 126.4 (2C), 125.2, 125.1, 123.4, 121.2, 117.5, 115.0, 113.6. MS: LC–MS (ESI) $^+$, found m/z 440 [$\text{M} + \text{H}$] $^+$:442.6 [$\text{M} + \text{H} + 2$] $^+$:444 [$\text{M} + \text{H} + 4$] $^+$ (9:3:1) (calculated for $\text{C}_{19}\text{H}_7\text{Cl}_3\text{F}_3\text{N}_3$, 438.97).

General Procedure for the Synthesis of Compounds 8–69.

Amine (2.0 equiv) was added to a stirred mixture of 6/7a,b (1.0 equiv) and triethylamine (2.0 equiv) in THF (10 mL). The mixture was irradiated in microwave reactor at 80 °C for 20 min, filtered hot, and allowed to cool. The solvent was removed in vacuo, and the residue was washed with a minimum amount of ice-cold ethanol. The resulting solid was recrystallized from acetone or ethanol to afford the target compound.

1-((2-(3-Hydroxypyrrolidin-1-yl)ethyl)amino)-3-(4-(trifluoromethyl)phenyl)benzo[4,5]imidazo[1,2-a]pyridine-4-carbonitrile 11. Yellow solid (53%). $R_f = 0.3$ (8% MeOH–DCM). Mp 267–269 °C. ^1H NMR (600 MHz, DMSO- d_6) δ 8.39 (d, $J = 8.4$ Hz, 1H), 7.98 (d, $J = 9.1$ Hz, 2H), 7.98 (d, $J = 9.1$ Hz, 2H), 7.87 (d, $J = 8.1$ Hz, 1H), 7.58 (t, $J = 8.1$ Hz, 1H), 7.39 (t, $J = 8.1$ Hz, 1H), 6.28 (s, 1H), 4.80 (br s, 1H), 4.27 (m, 1H), 3.65 (t, $J = 6.2$ Hz, 2H), 2.90 (m, 2H), 2.84 (m, 2H), 2.58 (m, 2H), 2.07 (m, 1H), 1.64 (m, 1H). ^{13}C NMR (150 MHz, DMSO- d_6) δ 150.6, 149.3, 149.0, 145.4, 141.8, 130.3, 130.0, 128.3, 126.4, 126.0, 125.4 (2C), 123.6 (2C), 121.2, 119.0, 117.6, 114.8, 90.7, 69.8, 62.8, 53.3, 52.5, 41.8, 34.9. LC–MS (ESI) $^+$, found $m/z = 466.1$ [$\text{M} + \text{H}$] $^+$ (calculated for $\text{C}_{25}\text{H}_{22}\text{F}_3\text{N}_5\text{O}$, 465.48). HPLC purity 99% ($t_R = 4.09$ min).

1-((5-(Diethylamino)pentan-2-yl)amino)-3-(4-(trifluoromethyl)phenyl)benzo[4,5]imidazo[1,2-a]pyridine-4-carbonitrile 17. Yellow solid (50%). $R_f = 0.3$ (10% MeOH–DCM). Mp 220–222 °C. ^1H NMR (400 MHz, DMSO- d_6) δ 8.42 (d, $J = 8.3$ Hz, 1H), 7.96 (m, 4H), 7.85 (d, $J = 8.0$ Hz, 1H), 7.58 (t, $J = 7.7$ Hz, 1H), 7.39 (t, $J = 7.3$ Hz, 1H), 6.31 (s, 1H), 4.03 (m, 1H), 2.48 (m, 6H), 1.92 (m, 1H), 1.65 (m, 3H), 1.38 (d, $J = 6.3$ Hz, 3H), 0.91 (t, $J = 7.0$ Hz, 6H). ^{13}C NMR (100 MHz, DMSO- d_6) δ 150.5, 149.6, 149.1 (2C), 145.4, 142.0, 130.3, 130.0 (2C), 128.6, 126.3, 126.0 (2C), 123.1, 120.6, 118.8, 117.6, 115.8, 91.3, 52.1, 50.0, 46.6 (2C), 33.7, 23.5, 20.1 (2C), 11.5. LC–MS (ESI) $^+$, found $m/z = 494.4$ [$\text{M} + \text{H}$] $^+$, (calculated for $\text{C}_{28}\text{H}_{30}\text{F}_3\text{N}_5$, 493.58). HPLC purity 98% ($t_R = 3.69$ min).

1-((N-Methylpiperidin-4-yl)amino)-3-(4-(trifluoromethyl)phenyl)benzo[4,5]imidazo[1,2-a]pyridine-4-carbonitrile 20. Yellow solid (51%). $R_f = 0.4$ (10% MeOH–DCM). Mp 215–217 °C. ^1H NMR (400 MHz, DMSO) δ 8.41 (d, $J = 8.3$ Hz, 1H), 7.96 (s, 4H), 7.85 (d, $J = 8.1$ Hz, 1H), 7.58 (t, $J = 7.7$ Hz, 1H), 7.40 (t, $J = 7.4$ Hz, 1H), 6.34 (s, 1H), 3.83 (m, 1H), 2.84 (m, 2H), 2.24 (s, 3H), 2.17 (t, $J = 10.6$ Hz, 2H), 2.07 (m, 2H), 1.92 (t, $J = 9.6$ Hz, 2H). ^{13}C NMR (101 MHz, DMSO) δ 150.6, 149.6, 148.9, 145.4, 142.0, 141.9, 130.3, 130.2, 130.0, 128.7, 128.6, 126.4, 126.2, 126.1, 126.0, 120.7, 118.8, 117.7, 117.6, 116.1, 91.6, 54.4, 50.7, 46.3, 31.1. LC–MS (ESI) $^+$, found $m/z = 450.2$ [$\text{M} + \text{H}$] $^+$ (calculated for $\text{C}_{25}\text{H}_{22}\text{F}_3\text{N}_5$, 449.48). HPLC purity 99% ($t_R = 4.03$ min).

3-(3,4-Dichlorophenyl)-1-((2-(ethylamino)ethyl)amino)benzo[4,5]imidazo[1,2-a]pyridine-4-carbonitrile 45. Yellow solid (29%). $R_f = 0.1$ (5% MeOH/DCM). Mp 235–237 °C. ^1H NMR (400 MHz, DMSO- d_6) δ 8.52 (d, $J = 8.1$ Hz, 1H), 7.96 (s, 1H), 7.83 (d, $J = 8.3$ Hz, 1H), 7.77 (d, $J = 7.9$ Hz, 1H), 7.71 (d, $J = 8.0$ Hz, 1H), 7.50 (t, $J = 7.6$ Hz, 1H), 7.30 (t, $J = 7.5$ Hz, 1H), 6.12 (s, 1H), 3.64 (t, $J = 6.2$ Hz, 2H), 3.07 (t, $J = 5.6$ Hz, 2H), 2.80 (q, $J = 8.0$ Hz, 2H), 1.13 (t, $J = 7.0$ Hz, 3H). ^{13}C NMR (100 MHz, DMSO- d_6) δ 150.0, 148.5, 145.4, 138.9, 132.5, 131.8, 131.1, 130.9, 129.3, 129.0 (2C), 125.7, 120.3, 118.5, 118.3 (2C), 115.4, 90.5, 47.2, 43.1 (2C), 14.3. LC–MS (ESI) $^+$, found $m/z = 424.2$ [$\text{M} + \text{H}$] $^+$:426.5 [$\text{M} + \text{H} + 2$] $^+$ (3:1) (calculated for $\text{C}_{22}\text{H}_{19}\text{Cl}_2\text{N}_5$, 423.10). HPLC purity 99% ($t_R = 3.53$ min).

9-Chloro-1-((2-(ethylamino)ethyl)amino)-3-(4-(trifluoromethyl)phenyl)benzo[4,5]imidazo[1,2-a]pyridine-4-carbonitrile 57. Yellow solid (36%). $R_f = 0.2$ (6% MeOH–DCM). Mp 223–225 °C. ^1H NMR (400 MHz, DMSO- d_6) δ 8.69 (d, $J = 8.7$ Hz, 1H), 7.90 (m, 4H), 7.44 (d, $J = 7.4$ Hz, 1H), 7.13 (t, $J = 8.0$ Hz, 1H), 5.83 (s, 1H), 3.58 (t, $J = 6.2$ Hz, 2H), 3.18 (t, $J = 6.2$ Hz, 2H), 2.94 (q, $J = 7.2$ Hz, 2H), 1.18 (t, $J = 7.2$ Hz, 3H). ^{13}C NMR (100 MHz, DMSO- d_6) δ 152.2, 151.9, 148.6, 143.5, 142.5, 131.5, 129.7, 129.4, 126.0, 125.8, 125.7, 124.2, 123.3, 120.3, 120.1, 119.5, 115.4 (2C), 72.8, 48.0, 44.4, 43.0, 12.9. LC–MS (ESI) $^+$, found $m/z = 458.3$ [$\text{M} + \text{H}$] $^+$:460.5 [$\text{M} + \text{H} + 2$] $^+$ (3:1) (calculated for $\text{C}_{23}\text{H}_{19}\text{ClF}_3\text{N}_5$, 457.13). HPLC purity 98% ($t_R = 3.52$ min).

7,8-Dichloro-1-((2-(ethylamino)ethyl)amino)-3-(4-(trifluoromethyl)phenyl)benzo[4,5]imidazo[1,2-a]pyridine-4-carbonitrile 59. Yellow solid (47%). $R_f = 0.4$ (8% MeOH–DCM). Mp 266–268 °C. ^1H NMR (600 MHz, DMSO- d_6) δ 8.92 (s, 1H), 7.85 (d, $J = 8.8$ Hz, 2H), 7.84 (d, $J = 8.4$ Hz, 2H), 7.72 (s, 1H), 5.72 (s, 1H), 3.60 (t, $J = 6.2$ Hz, 2H), 3.23 (t, $J = 6.2$ Hz, 2H), 3.03 (q, $J = 7.3$ Hz, 2H), 1.24 (t, $J = 7.3$ Hz, 3H). ^{13}C NMR (150 MHz, DMSO- d_6) δ 154.1, 152.4, 148.1, 145.5, 143.8, 130.2, 129.6 (2C), 129.5, 129.3, 126.3, 125.6, 123.7, 120.3, 119.9, 117.6 (2C), 116.7, 91.6, 48.1, 44.7, 42.9, 12.2. LC–MS (ESI) $^+$, found $m/z = 492.2$ [$\text{M} + \text{H}$] $^+$:494.4 [$\text{M} + \text{H} + 2$] $^+$:496.5 [$\text{M} + \text{H} + 4$] $^+$ (9:3:1) (calculated for $\text{C}_{23}\text{H}_{18}\text{Cl}_2\text{F}_3\text{N}_5$, 491.09). HPLC purity 98% ($t_R = 4.29$ min).

7,9-Dichloro-1-((2-(ethylamino)ethyl)amino)-3-(4-(trifluoromethyl)phenyl)benzo[4,5]imidazo[1,2-a]pyridine-4-carbonitrile 60. Yellow solid (42%). $R_f = 0.3$ (8% MeOH–DCM). Mp 277–279 °C. ^1H NMR (600 MHz, DMSO- d_6) δ 8.81 (d, $J = 2.0$ Hz, 1H), 7.86 (d, $J = 8.4$ Hz, 2H), 7.83 (d, $J = 8.2$ Hz, 2H), 7.43 (d, $J = 2.0$ Hz, 1H), 5.67 (s, 1H), 3.57 (t, $J = 6.2$ Hz, 2H), 3.26 (t, $J = 6.2$ Hz, 2H), 3.06 (q, $J = 7.2$ Hz, 2H), 1.24 (t, $J = 7.2$ Hz, 3H). ^{13}C NMR (150 MHz, DMSO- d_6) δ 153.9, 152.9, 147.7, 144.0, 141.6, 132.2, 129.6 (2C), 129.2, 125.7, 125.6, 123.7 (2C), 123.1, 121.8, 120.8, 119.6, 115.6, 91.9, 48.1, 44.9, 42.7, 11.8. LC–MS (ESI) $^+$, found $m/z = 492.2$ [$\text{M} + \text{H}$] $^+$:494.4 [$\text{M} + \text{H} + 2$] $^+$:496.5 [$\text{M} + \text{H} + 4$] $^+$ (9:3:1) (calculated for $\text{C}_{23}\text{H}_{18}\text{Cl}_2\text{F}_3\text{N}_5$, 491.09). HPLC purity 99% ($t_R = 4.26$ min).

6-((2-(Ethylamino)ethyl)amino)-8-(4-(trifluoromethyl)phenyl)imidazo[1,2-a:4,5-b']dipyridine-9-carbonitrile 64. Yellow solid (32%). $R_f = 0.3$ (10% MeOH–DCM). Mp 225–227 °C. ^1H NMR (400 MHz, DMSO- d_6) δ 8.41 (dd, $J = 4.8, 1.4$ Hz, 1H), 8.26 (dd, $J = 8.2, 1.4$ Hz, 1H), 7.95 (m, 4H), 7.64 (dd, $J = 8.2, 4.8$ Hz, 1H), 6.33 (s, 1H), 3.67 (t, $J = 6.0$ Hz, 2H), 2.94 (t, $J = 6.0$ Hz, 2H), 2.65 (q, $J = 7.1$ Hz, 2H), 1.08 (t, $J = 7.1$ Hz, 3H). ^{13}C NMR (100 MHz, DMSO- d_6) δ 152.3, 149.2, 149.0, 144.1, 141.9, 140.3, 137.8, 130.4, 130.0 (2C), 126.5, 126.0 (2C), 122.2 (3C), 117.3, 90.1, 47.4, 43.5, 42.7, 15.6. LC–MS (ESI) $^+$, found $m/z = 425.2$ [$\text{M} + \text{H}$] $^+$ (calculated for $\text{C}_{22}\text{H}_{19}\text{F}_3\text{N}_6$, 424.43). HPLC purity 96% ($t_R = 3.25$ min).

2-Fluoro-1-((2-(3-hydroxypyrrolidin-1-yl)ethyl)amino)-3-(4-(trifluoromethyl)phenyl)benzo[4,5]imidazo[1,2-a]pyridine-4-carbonitrile 69. Yellow solid (44%). $R_f = 0.3$ (5% MeOH–DCM). Mp 265–267 °C. ^1H NMR (400 MHz, DMSO- d_6) δ 8.54 (d, $J = 8.4$ Hz, 1H), 7.96 (d, $J = 8.0$ Hz, 2H), 7.86 (d, $J = 8.0$ Hz, 2H), 7.82 (d, $J = 8.2$ Hz, 1H), 7.55 (t, $J = 7.8$ Hz, 1H), 7.34 (t, $J = 7.8$ Hz, 1H), 4.30 (m, 1H), 3.87 (m, 2H), 2.98 (m, 2H), 2.92 (m, 2H), 2.69 (m, 2H), 2.10 (m, 1H), 1.70 (m, 1H). ^{13}C NMR (100 MHz, DMSO- d_6) δ 147.2, 145.6, 141.3, 141.0, 136.5, 133.0, 130.9, 130.1 (2C), 126.1, 125.8 (2C), 120.6, 118.7, 117.2, 117.1, 115.5, 69.8, 62.5, 55.4, 55.3, 52.4, 44.3, 44.2, 34.7. LC–MS (ESI) $^+$, found $m/z = 484.2$ [$\text{M} + \text{H}$] $^+$ (calculated for $\text{C}_{25}\text{H}_{21}\text{F}_4\text{N}_5\text{O}$, 483.17). HPLC purity 99% ($t_R = 3.51$ min).

■ ASSOCIATED CONTENT**Supporting Information**

The Supporting Information is available free of charge on the ACS Publications website at DOI: [10.1021/acs.jmedchem.6b01641](https://doi.org/10.1021/acs.jmedchem.6b01641).

Molecular formula strings and some data (CSV)

Characterization of all intermediates and final compounds, details of assay procedures and further descriptions of the biological experiments (cytotoxicity analysis, in vitro determination of antiplasmodial activity, in vivo efficacy experiments, in vitro gametocytocidal experiments, liver stage assays and killing kinetics), in vitro ADME assays (kinetic solubility and artificial membrane permeability experiments), metabolic stability experiments and determination of mechanism of action (in vitro β -hematin, heme fractionation assays, and prediction of vacuolar accumulation) (PDF)

AUTHOR INFORMATION

Corresponding Author

*Phone: +27-21-6502557. Fax: +27-21-6505195. E-mail: Kelly.Chibale@uct.ac.za.

ORCID

Timothy J. Egan: 0000-0001-7720-8473

Kelly Chibale: 0000-0002-1327-4727

Notes

The authors declare no competing financial interest.

ACKNOWLEDGMENTS

The University of Cape Town, South African Medical Research Council (SAMRC), and South African Research Chairs Initiative of the Department of Science and Technology, administered through the South African National Research Foundation, are gratefully acknowledged for support (K.C.). The SAMRC is further acknowledged for support (L.-M.B., T.L.C. and T.J.E.).

ABBREVIATIONS USED

SAR, structure–activity relationship; ADME, absorption, distribution, metabolism, and excretion; CQ, chloroquine; po, oral administration; iv, intravenous administration; MSD, mean survival days; PK, pharmacokinetics; PBI, pyrido[1,2-*a*]-benzimidazole; BHIA, β -hematin inhibition assay; LG, late gametocyte; EG, early gametocyte

REFERENCES

- (1) World Health Organization (WHO). World Malaria Report 2015. <http://www.who.int/malaria/publications/world-malaria-report-2015/report/en/> (accessed September 24, 2016).
- (2) Prudencio, M.; Rodriguez, A.; Mota, M. M. The Silent Path to Thousands of Merozoites: The Plasmodium Liver Stage. *Nat. Rev. Microbiol.* **2006**, *4*, 849–856.
- (3) Dondorp, A. M.; Nosten, F.; Yi, P.; Das, D.; Phyto, A. P.; Tarning, J.; Lwin, K. M.; Ariey, F.; Hanpithakpong, W.; Lee, S. J.; Ringwald, P.; Silamut, K.; Imwong, M.; Chotivanich, K.; Lim, P.; Herdman, T.; An, S. S.; Yeung, S.; Singhasivanon, P.; Day, N. P.; Lindegardh, N.; Socheat, D.; White, N. J. Artemisinin Resistance in Plasmodium falciparum Malaria. *N. Engl. J. Med.* **2009**, *361*, 455–467.
- (4) Noedl, H.; Se, Y.; Schaefer, K.; Smith, B. L.; Socheat, D.; Fukuda, M. M. Evidence of Artemisinin-resistant Malaria in western Cambodia. *N. Engl. J. Med.* **2008**, *359*, 2619–2620.
- (5) Horton, D. A.; Bourne, G. T.; Smythe, M. L. The Combinatorial Synthesis of Bicyclic Privileged Structures or Privileged Substructures. *Chem. Rev.* **2003**, *103*, 893–930.
- (6) Camacho, J.; Barazarte, A.; Gamboa, N.; Rodrigues, J.; Rojas, R.; Vaisberg, A.; Gilman, R.; Charris, J. Synthesis and Biological Evaluation of Benzimidazole-5-carbohydrazide Derivatives as Antimalarial, Cytotoxic and Antitubercular Agents. *Bioorg. Med. Chem.* **2011**, *19*, 2023–2029.
- (7) Keri, R. S.; Hiremathad, A.; Budagumpi, S.; Nagaraja, B. M. Comprehensive Review in Current Developments of Benzimidazole-Based Medicinal Chemistry. *Chem. Biol. Drug Des.* **2015**, *86*, 19–65.
- (8) Keurulainen, L.; Vahermo, M.; Puente-Felipe, M.; Sandoval-Izquierdo, E.; Crespo-Fernandez, B.; Guijarro-Lopez, L.; Huertas-Valentin, L.; de las Heras-Duena, L.; Leino, T. O.; Siiskonen, A.; Balcells-Pages, L.; Sanz, L. M.; Castaneda-Casado, P.; Jimenez-Diaz, M. B.; Martinez-Martinez, M. S.; Viera, S.; Kiuru, P.; Calderon, F.; Yli-Kauhala, J. A. Developability-Focused Optimization Approach Allows Identification of in Vivo Fast-Acting Antimalarials: N-[3-[(Benzimidazol-2-yl)amino]propyl]amides. *J. Med. Chem.* **2015**, *58*, 4573–4580.
- (9) Saify, Z. S.; Azim, M. K.; Ahmad, W.; Nisa, M.; Goldberg, D. E.; Hussain, S. A.; Akhtar, S.; Akram, A.; Arayne, A.; Oksman, A.; Khan, I.

A. New Benzimidazole Derivatives as Antiplasmodial Agents and Plasmepsin Inhibitors: Synthesis and Analysis of Structure-Activity Relationships. *Bioorg. Med. Chem. Lett.* **2012**, *22*, 1282–1286.

- (10) Rida, S. M.; Soliman, F. S. G.; Badawey, E.-S. A. M.; El-Ghazzawi, E.; Kader, O.; Kappe, T. Benzimidazole Condensed Ring Systems. 1. Syntheses and Biological Investigations of Some Substituted Pyrido[1,2-*a*]benzimidazoles. *J. Heterocycl. Chem.* **1988**, *25*, 1087–1093.

- (11) Ndakala, A. J.; Gessner, R. K.; Gitari, P. W.; October, N.; White, K. L.; Hudson, A.; Fakorede, F.; Shackelford, D. M.; Kaiser, M.; Yeates, C.; Charman, S. A.; Chibale, K. Antimalarial Pyrido[1,2-*a*]benzimidazoles. *J. Med. Chem.* **2011**, *54*, 4581–4589.

- (12) Ishikawa, M.; Hashimoto, Y. Improvement in Aqueous Solubility in Small Molecule Drug Discovery Programs by Disruption of Molecular Planarity and Symmetry. *J. Med. Chem.* **2011**, *54*, 1539–1554.

- (13) Reader, J.; Botha, M.; Theron, A.; Lauterbach, S. B.; Rossouw, C.; Engelbrecht, D.; Wepener, M.; Smit, A.; Leroy, D.; Mancama, D.; Coetzer, T. L.; Birkholtz, L. M. Nowhere to Hide: Interrogating Different Metabolic Parameters of Plasmodium falciparum Gametocytes in a Transmission-blocking Drug Discovery Pipeline Towards Malaria Elimination. *Malar. J.* **2015**, *14*, 213.

- (14) Prudencio, M.; Mota, M. M.; Mendes, A. M. A Toolbox to Study Liver Stage Malaria. *Trends Parasitol.* **2011**, *27*, 565–574.

- (15) Ploemen, I. H.; Prudencio, M.; Douradinha, B. G.; Ramesar, J.; Fonager, J.; van Gemert, G. J.; Luty, A. J.; Hermsen, C. C.; Sauerwein, R. W.; Baptista, F. G.; Mota, M. M.; Waters, A. P.; Que, L.; Lowik, C. W.; Khan, S. M.; Janse, C. J.; Franke-Fayard, B. M. Visualisation and Quantitative Analysis of the Rodent Malaria Liver Stage by Real Time Imaging. *PLoS One* **2009**, *4*, e7881.

- (16) Carrasco, M. P.; Machado, M.; Goncalves, L.; Sharma, M.; Gut, J.; Lukens, A. K.; Wirth, D. F.; Andre, V.; Duarte, M. T.; Guedes, R. C.; Dos Santos, D. J.; Rosenthal, P. J.; Mazitschek, R.; Prudencio, M.; Moreira, R. Probing the Azaaurone Scaffold against the Hepatic and Erythrocytic Stages of Malaria Parasites. *ChemMedChem* **2016**, *11*, 2194–2204.

- (17) Vale, N.; Moreira, R.; Gomes, P. Primaquine Revisited Six Decades After Its Discovery. *Eur. J. Med. Chem.* **2009**, *44*, 937–953.

- (18) Le Manach, C.; Scheurer, C.; Sax, S.; Schleiferbock, S.; Cabrera, D. G.; Younis, Y.; Paquet, T.; Street, L.; Smith, P.; Ding, X. C.; Waterson, D.; Witty, M. J.; Leroy, D.; Chibale, K.; Wittlin, S. Fast In Vitro Methods to Determine The Speed of Action and the Stage-specificity of Anti-malarials in Plasmodium falciparum. *Malar. J.* **2013**, *12*, 424–430.

- (19) Combrinck, J. M.; Mabothe, T. E.; Ncozaki, K. K.; Ambele, M. A.; Taylor, D.; Smith, P. J.; Hoppe, H. C.; Egan, T. J. Insights Into The Role of Heme in the Mechanism of Action of Antimalarials. *ACS Chem. Biol.* **2013**, *8*, 133–137.

- (20) Wicht, K. J.; Combrinck, J. M.; Smith, P. J.; Hunter, R.; Egan, T. J. Identification and SAR Evaluation of Hemozoin-inhibiting Benzamides Active Against Plasmodium falciparum. *J. Med. Chem.* **2016**, *59*, 6512–6530.

- (21) de Villiers, K. A.; Gildenhuis, J.; le Roex, T. Iron(III)-Protoporphyrin IX Complexes of the Antimalarial Cinchona Alkaloids Quinine and Quinidine. *ACS Chem. Biol.* **2012**, *7*, 666–671.

- (22) de Villiers, K. A.; Marques, H. M.; Egan, T. J. The Crystal Structure of Halofantrine-Ferriprotoporphyrin IX and the Mechanism of Action of Arylmethanol Antimalarials. *J. Inorg. Biochem.* **2008**, *102*, 1660–1667.

- (23) Lyons, D. M.; Huttunen, K. M.; Browne, K. A.; Ciccone, A.; Trapani, J. A.; Denny, W. A.; Spicer, J. A. Inhibition of the Cellular Function of Perforin by 1-amino-2,4-dicyanopyrido[1,2-*a*]-benzimidazoles. *Bioorg. Med. Chem.* **2011**, *19*, 4091–4100.

- (24) Wirth, C. C.; Glushakova, S.; Scheuermayer, M.; Repnik, U.; Garg, S.; Schaack, D.; Kachman, M. M.; Weissbach, T.; Zimmerberg, J.; Dandekar, T.; Griffiths, G.; Chitnis, C. E.; Singh, S.; Fischer, R.; Pradel, G. Perforin-like Protein PPLP2 Permeabilizes the Red Blood Cell Membrane During Egress of Plasmodium falciparum Gametocytes. *Cell. Microbiol.* **2014**, *16*, 709–733.

(25) Khare, S.; Roach, S. L.; Barnes, S. W.; Hoepfner, D.; Walker, J. R.; Chatterjee, A. K.; Neitz, R. J.; Arkin, M. R.; McNamara, C. W.; Ballard, J.; Lai, Y.; Fu, Y.; Molteni, V.; Yeh, V.; McKerrow, J. H.; Glynn, R. J.; Supek, F. Utilizing Chemical Genomics to Identify Cytochrome b as a Novel Drug Target for Chagas Disease. *PLoS Pathog.* **2015**, *11*, e1005058.

(26) Paquet, T.; Le Manach, C.; Cabrera, D. G.; Younis, Y.; Henrich, P.; Abraham, T.; Lee, M. C. S.; Basak, R.; Ghidelli-Disse, S.; Lafuente-Monasterio, M. J.; Bantscheff, M.; Ruecker, A.; Blagborough, A. M.; Zakutansky, S.; Zeeman, A.-M.; White, K. L.; Shackelford, D. M.; Mannila, J.; Morizzi, J.; Scheurer, C.; Angulo-Barturen, I.; Martínez, M. S.; Ferrer, S.; Sanz, L. M.; Gamo, F. J.; Reader, J.; Botha, M.; Dechering, K. J.; Sauerwein, R. W.; Tungtaeng, A.; Vanachayangkul, P.; Lim, C. S.; Burrows, J. N.; Witty, M. J.; Marsh, K. C.; Bodenreider, C.; Rochford, R.; Solapure, S. M.; Jiménez-Díaz, M. B.; Wittlin, S.; Charman, S. A.; Donini, C.; Campo, B.; Birkholtz, L.-M.; Hanson, K. K.; Drewes, G.; Kocken, C.; Delves, M. J.; Leroy, D.; Fidock, D. A.; Waterson, D.; Street, L. J.; Chibale, K. Target Identification and Elucidation of the Complete Life Cycle Fingerprint of the Novel Plasmodium PI4K inhibitor MMV390048. *Sci. Transl. Med.* **2017**, in press.

(27) Le Manach, C.; Gonzalez Cabrera, D.; Douelle, F.; Nchinda, A. T.; Younis, Y.; Taylor, D.; Wiesner, L.; White, K. L.; Ryan, E.; March, C.; Duffy, S.; Avery, V. M.; Waterson, D.; Witty, M. J.; Wittlin, S.; Charman, S. A.; Street, L. J.; Chibale, K. Medicinal Chemistry Optimization of Antiplasmodial Imidazopyridazine Hits From High Throughput Screening of a SoftFocus Kinase Library: Part 1. *J. Med. Chem.* **2014**, *57*, 2789–2798.